

5-23-2016

Hydrodynamics of compartmented fluidized beds for concentrated solar power applications

Roberto Solimene

Consiglio Nazionale delle Ricerche/Istituto di Ricerche sulla Combustione, Italy, solimene@irc.cnr.it

Riccardo Chirone

Istituto di Ricerche sulla Combustione - Consiglio Nazionale delle Ricerche, Italy

Andrea Paulillo

Dipartimento di Ingegneria Chimica, dei Materiali e della Produzione Industriale - Università degli Studi di Napoli Federico II, Italy

Piero Salatino

Dipartimento di Ingegneria Chimica, dei Materiali e della Produzione Industriale - Università degli Studi di Napoli Federico II, Italy

Follow this and additional works at: http://dc.engconfintl.org/fluidization_xv



Part of the [Chemical Engineering Commons](#)

Recommended Citation

Roberto Solimene, Riccardo Chirone, Andrea Paulillo, and Piero Salatino, "Hydrodynamics of compartmented fluidized beds for concentrated solar power applications" in "Fluidization XV", Jamal Chaouki, Ecole Polytechnique de Montreal, Canada Franco Berruti, Wewstern University, Canada Xiaotao Bi, UBC, Canada Ray Cocco, PSRI Inc. USA Eds, ECI Symposium Series, (2016). http://dc.engconfintl.org/fluidization_xv/43

This Abstract and Presentation is brought to you for free and open access by the Proceedings at ECI Digital Archives. It has been accepted for inclusion in Fluidization XV by an authorized administrator of ECI Digital Archives. For more information, please contact franco@bepress.com.

HYDRODYNAMICS OF COMPARTMENTED FLUIDIZED BEDS FOR CONCENTRATED SOLAR POWER AND THERMAL ENERGY STORAGE APPLICATIONS

Simona Migliozzi*, Andrea Paulillo*, Riccardo Chirone**, Piero
Salatino*, Roberto Solimene**,

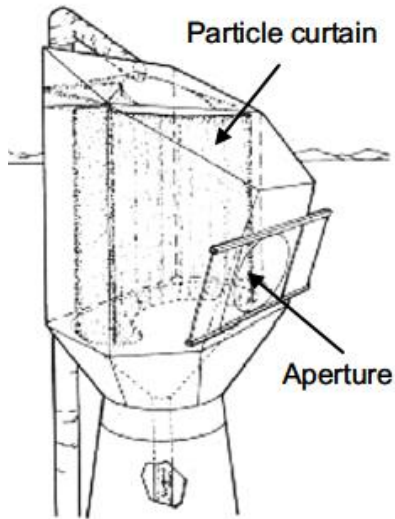
*Dipartimento di Ingegneria Chimica, dei Materiali e della Produzione Industriale,
Università degli Studi di Napoli Federico II

**Istituto di Ricerche sulla Combustione, Consiglio Nazionale delle Ricerche, Napoli

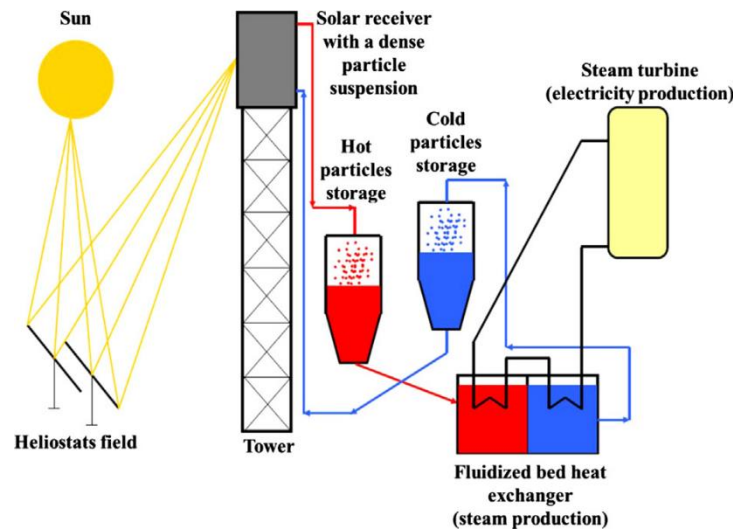


Particle receivers for CSP applications

Particle receivers are gaining much interest mainly for their potential of high temperature operation and as thermal energy storage



Falling particle receiver

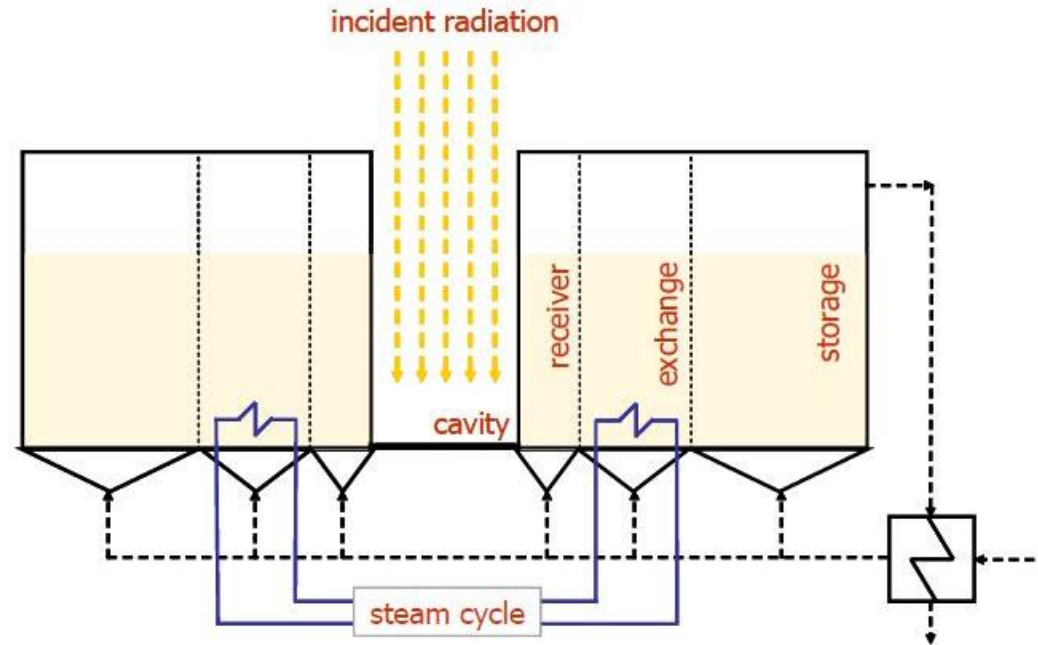


Dense gas-solid suspensions thanks to their excellent thermal properties

COMPARTMENTED DENSE GAS FLUIDIZED BEDS

System optimized to accomplish three complementary tasks:

- ❖ **RECEIVER:** Collection of highly concentrated (100-1000 suns) incident solar radiation
- ❖ **EXCHANGE:** heat transfer to the working fluid of the thermodynamic cycle
- ❖ **STORAGE:** thermal energy for equalizing the inherent time-variability of the incident solar radiation



Challenge: compartmented fluidization without physical confinements just by partitioning of the fluidizing gas to a compartmented distributor to preserve the fluidized bed thermal properties

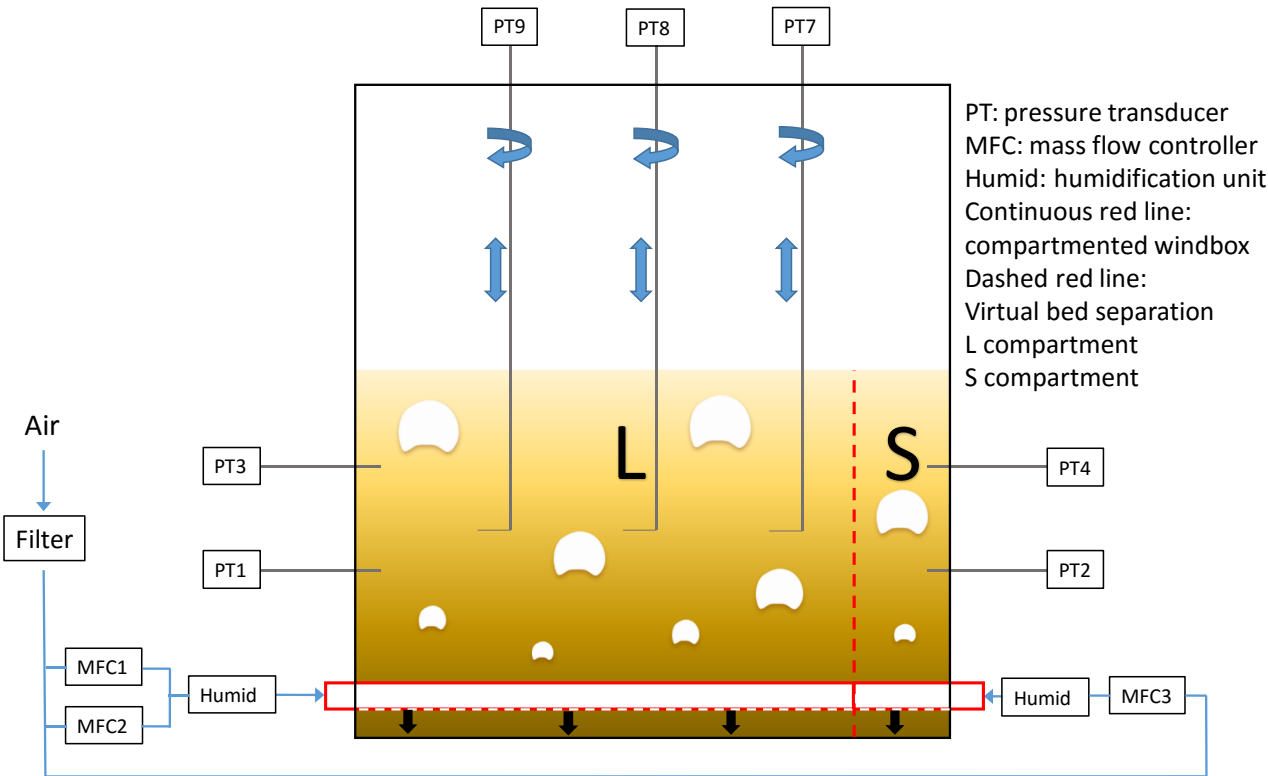
Aim of the work

The aim of this work was to study the hydrodynamics of a near-2D dense gas-fluidized bed operated at ambient conditions and equipped with a compartmented gas distributor.

Bed hydrodynamics under even and uneven fluidization conditions was characterized by:

- ✓ pressure measurements to mark the onset of local fluidization and to assess the location and extension of fluidized and defluidized regions
- ✓ space- and time-resolved void fraction profiles to analyze the dynamical patterns of the bubble and of the emulsion phases

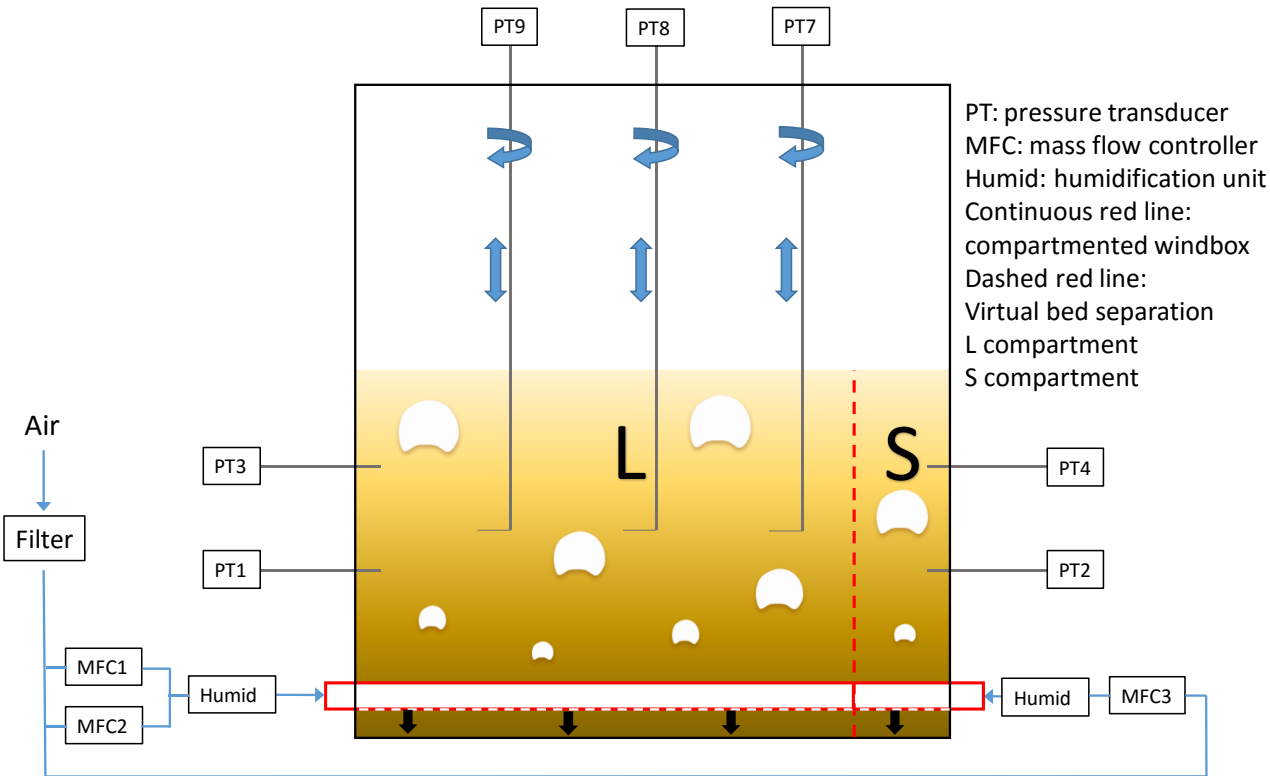
Experimental apparatus



- ✓ near-2D fluidized bed (2850x1860x200mm) with a thickness large enough to prevent extensive wall effects for bubbles smaller than 120 mm.
- ✓ two spargers acting as gas distributors intentionally of different length so to establish uneven bed fluidization with asymmetric patterns.
- ✓ the corresponding sections of the fluidized bed, as L (*long*), and S (*short*)

- ✓ Coordinate system (O,x,h):
 - ✓ origin O located on the side wall of the L compartment just above the L sparger
 - ✓ coordinate x represents the distance from the side wall of the L compartment
 - ✓ coordinate h represents the distance from the upper surface of the distributor
- ✓ Bed compartment L extending over $0 < x < 1480$ mm
- ✓ Bed compartment S extending over $1480 < x < 1860$ mm.

Diagnostics



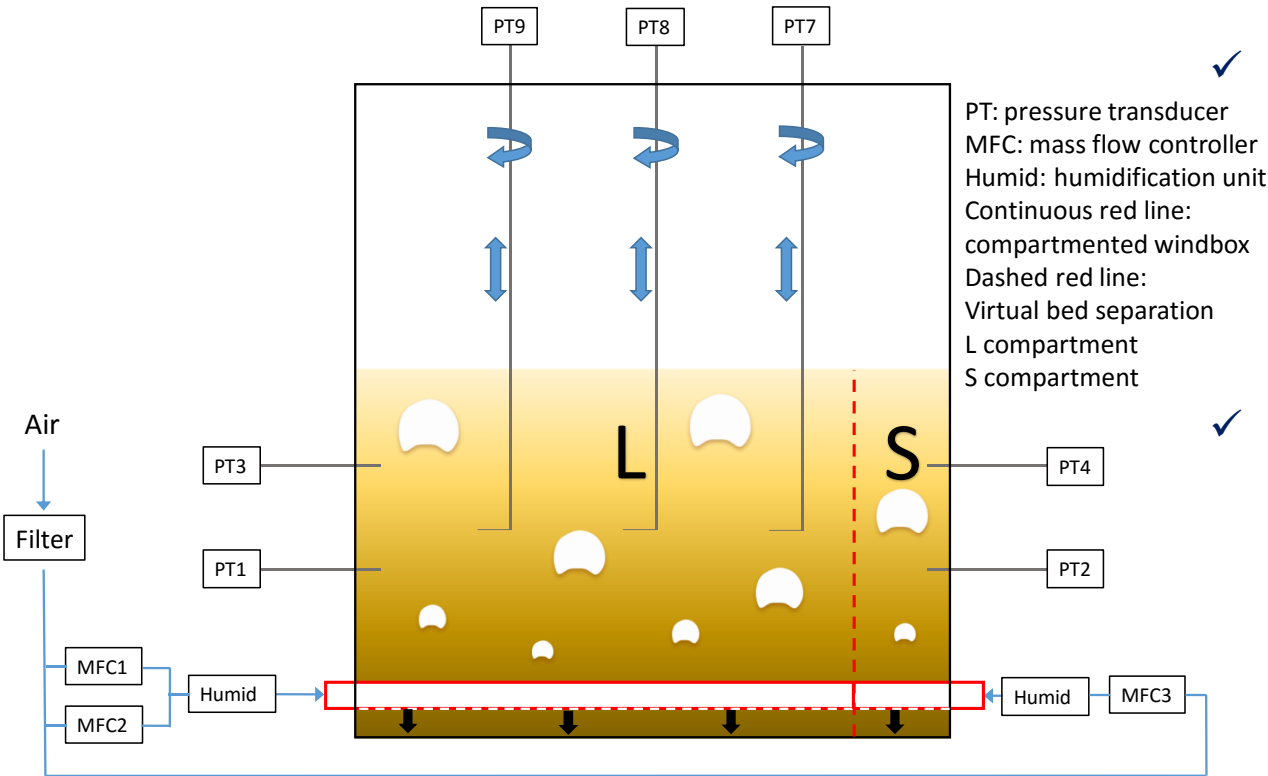
✓ three movable L-shaped probes were vertically immersed in the bulk of the bed to perform static gas pressure measurements at different levels above the distributor and at multiple locations by simply rotating the probe around its axis.

✓ The dynamical behavior of the fluidized bed under even and uneven fluidization conditions and at different vertical and horizontal positions was characterized by two needle-shaped custom-made capacitance probes in the proximity of the virtual bed separation between L and S compartments

- ✓ guarded-type sensor
- ✓ OD 1.5mm inner protruding electrode 7.5mm long
- ✓ OD 6.25mm outer electrode



Experimental procedure



✓ hydrodynamics of the fluidized bed under even and uneven fluidization conditions in order to verify the effectiveness of compartmented bed fluidization

✓ fluidizing gas flow rates to the L and S spargers was metered so as to operate one section as the “active” bed section ($U > U_{mf}$) while the other section was in a “passive” state ($0 \leq U < U_{mf}$)

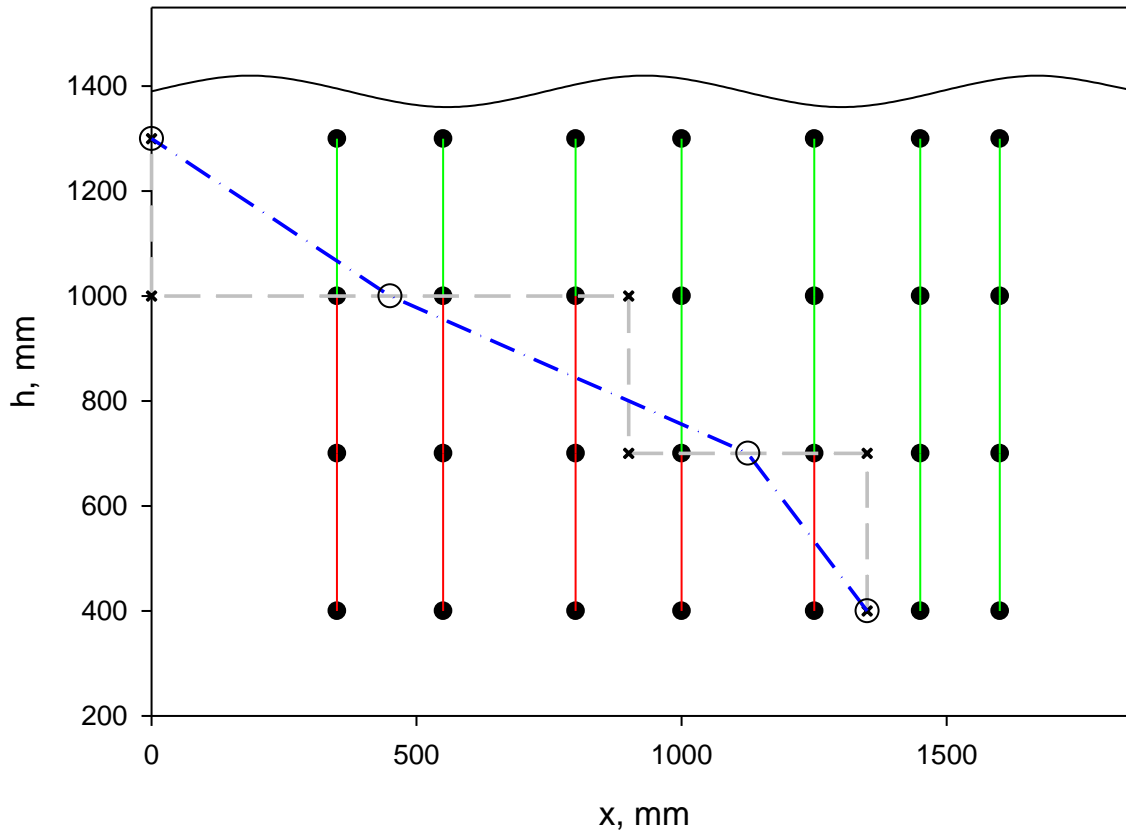
✓ static bed height $H_{bed} = 0.55, 1\text{m}, 1.39$ and 1.85m

✓ U_S and U_L ranging between 0 and $4 U_{mf}$

✓ fine silica sand ($145 \mu\text{m}$) to have large heat transfer coefficient and effective thermal diffusivity even at small fluidization velocities

✓ Sections S and L could be interchanged in the role of “active” and “passive” sections, so that the influence of relative lateral size of the “active” and “passive” sections could be assessed

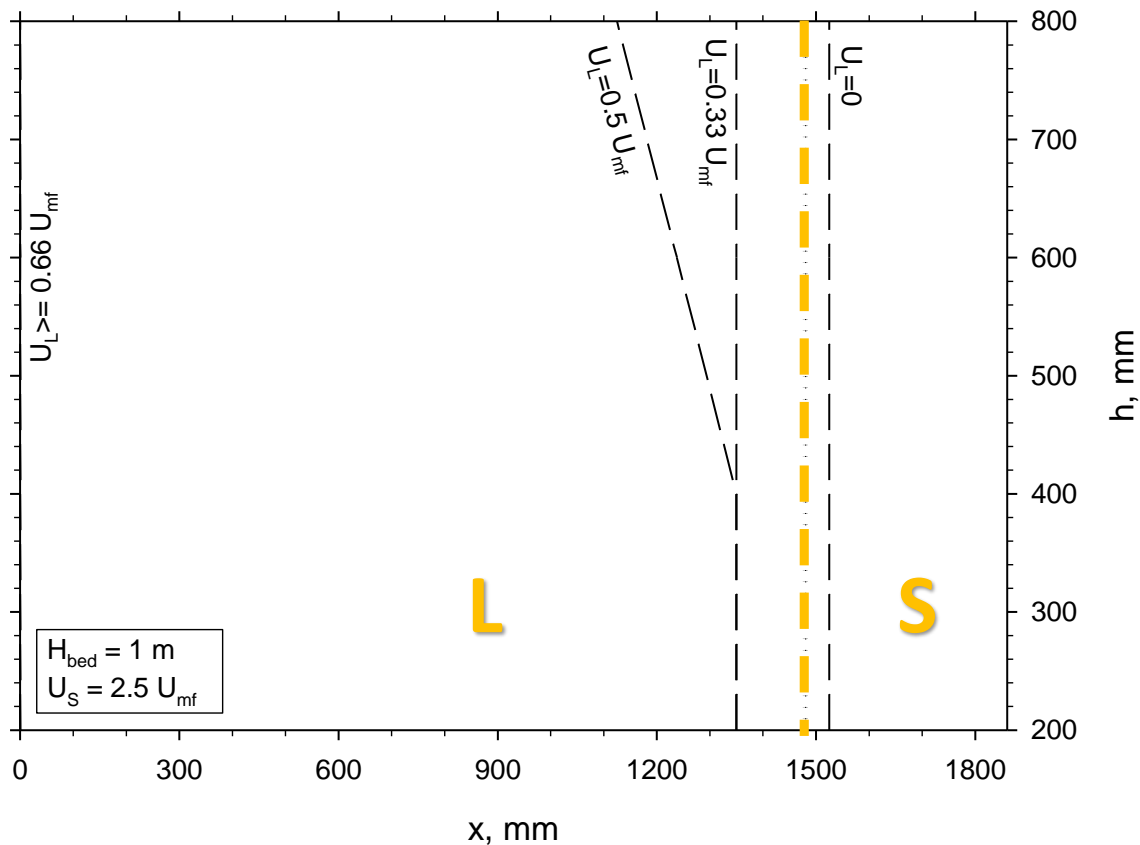
Fluidization maps



- ✓ Black points: location of the pressure taps.
- ✓ pressure gradients between adjacent taps located on the same x
- ✓ A pressure gradient exceeding a threshold of 0.11mbar/mm (90% of that corresponding to minimum fluidization condition) was assumed to mark the onset of local fluidization.
- ✓ red line: the bed is locally de-fluidized
- ✓ green line: the bed is locally fluidized
- ✓ Blue line: the boundaries between fluidized and de-fluidized regions

Fluidization maps

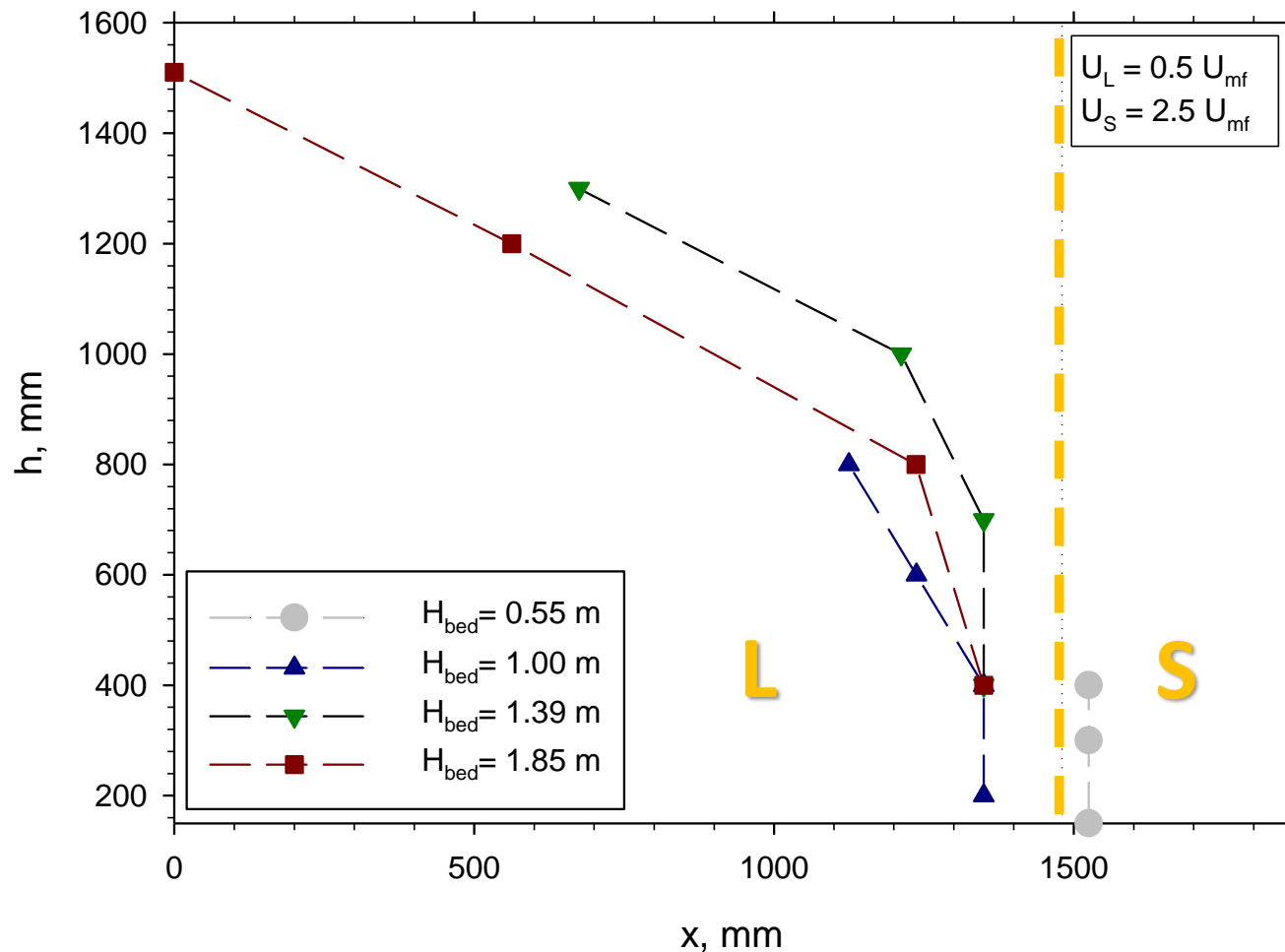
S compartment is active



- ✓ Separation boundaries between fluidized and de-fluidized regions are reported as black dashed lines: the fluidized bed region lies to the right of the separation boundary
- ✓ effective compartmentation at $U_L < 0.33 U_{mf}$
- ✓ For $0.33 U_{mf} < U_L < 0.66 U_{mf}$ the fluidized region extends also to part of the passive L compartment owing to gas crossflow from the active S zone to the passive L zone
- ✓ $U_L > 0.66 U_{mf}$, the entire bed is in the fluidized state

Fluidization maps

S compartment is active

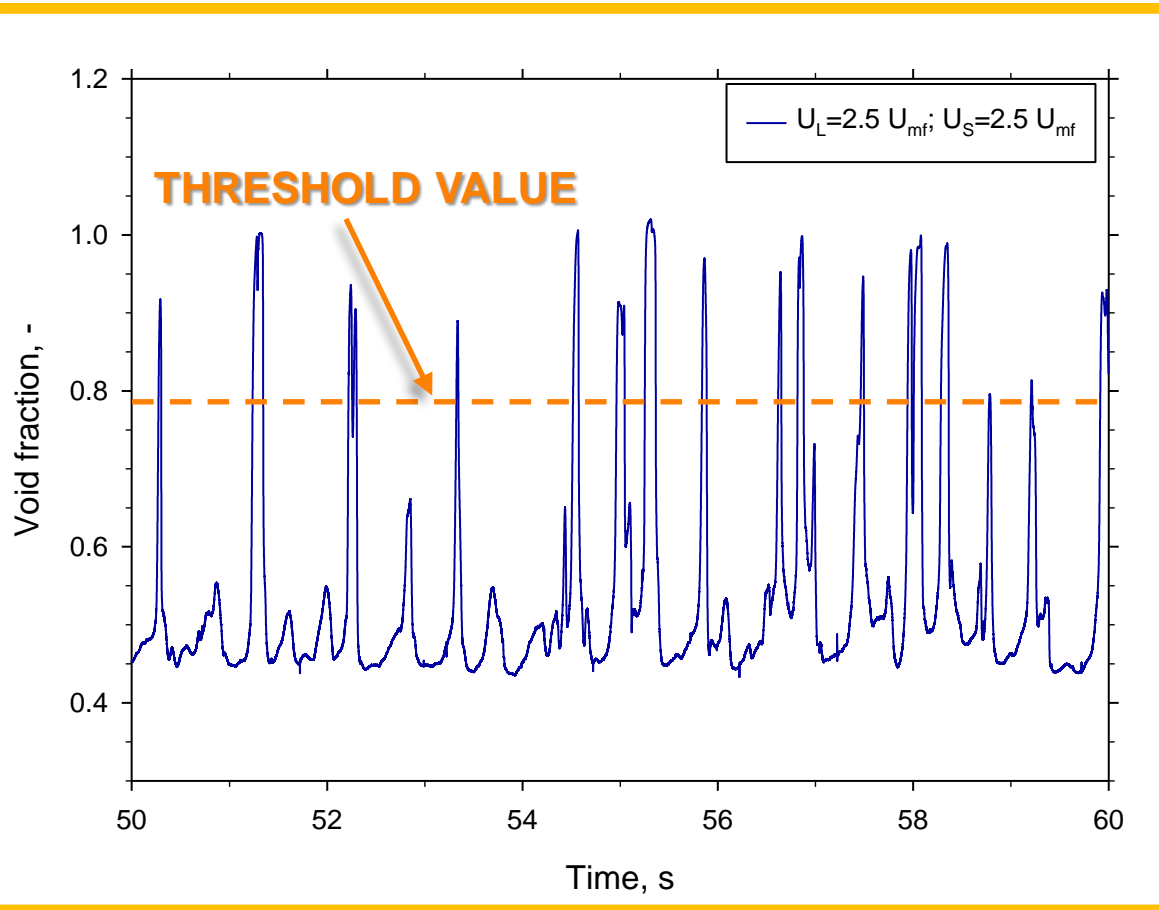


✓ A second series of maps refers to experiments carried out with a fixed value of gas flow rates to the passive and active section for different values of the static bed height.

✓ Effective compartmented fluidized bed for shallow bed

✓ the boundary between the fluidized and non-fluidized regions reported for different static bed height does not significantly change

Time-resolved void fraction signals



✓ Following the method developed by Molerus and Werther, the signal can be deconvoluted in a bubble-related component superimposed to the component associated with voidage fluctuations in the emulsion phase.

✓ Bubble phase properties:

- ✓ mean bubble frequency (k)
- ✓ the mean bubble rise velocity (v_{br})
- ✓ mean bubble pierced length, (l_b)

✓ mobility of dense phase:

- ✓ standard deviation
- ✓ dominant frequency by power spectrum density

$$D = \frac{1}{3\sqrt{8}} \frac{\langle v \rangle d_p}{\epsilon_s}$$

$$\langle v \rangle = \frac{\sigma_{cv} V_C f}{S_C}$$

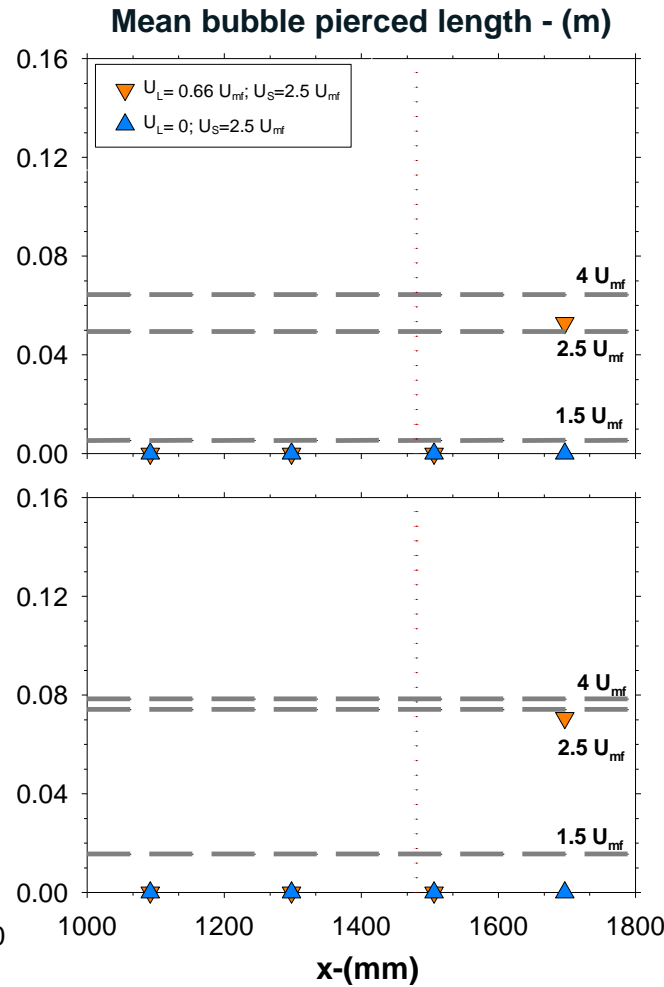
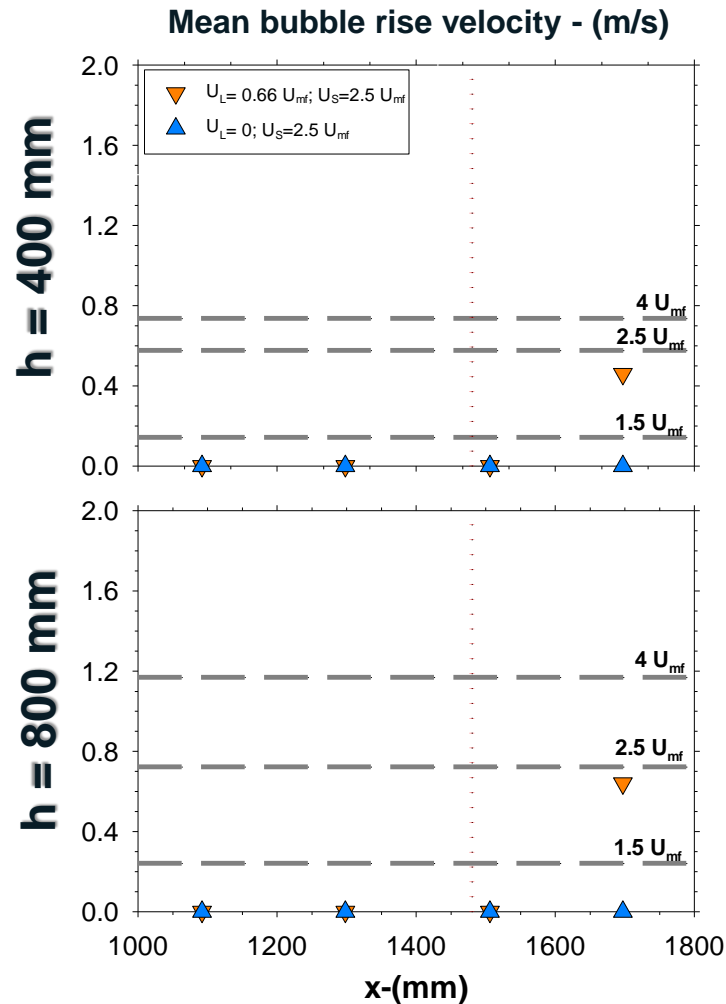
Bubble phase properties

S compartment is active ($H_{bed} = 1\text{ m}$)

✓ moderately uneven fluidization, corresponding to the minimum fluidizing gas velocity necessary to fluidize the whole bed:

✓ effective bed compartmentation, except nearby the virtual bed separation between the compartments

✓ strongly uneven fluidization, corresponding to setting to 0 the gas superficial velocity in the passive zone
 ✓ no bubble phase

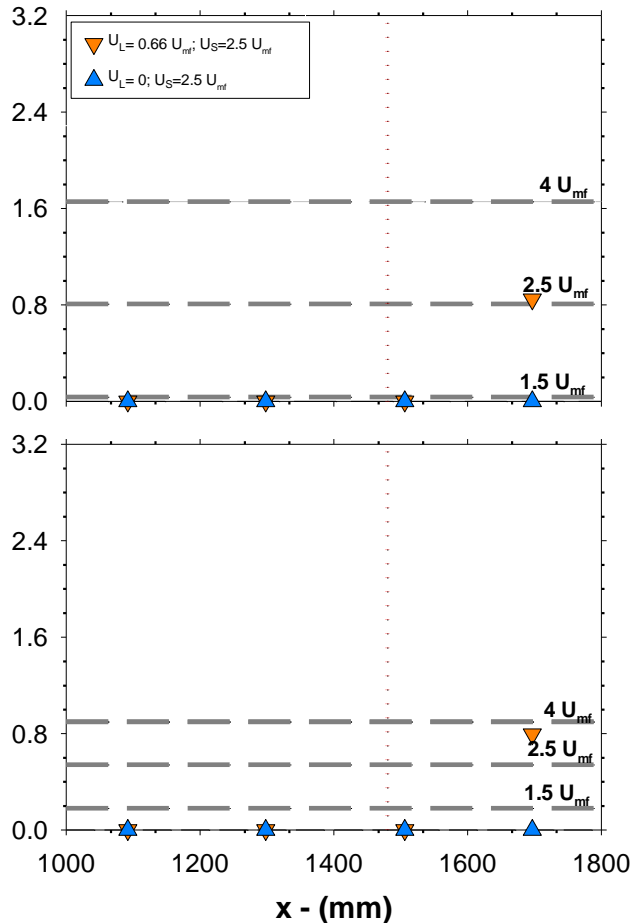


Bubble and dense phase properties

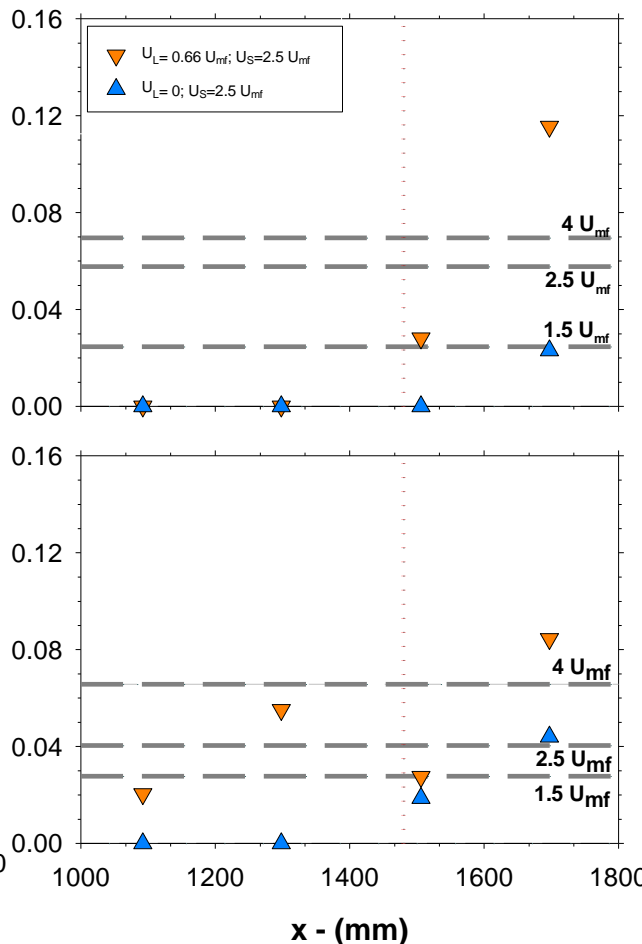
S compartment is active ($H_{bed} = 1\text{ m}$)

$h = 400\text{ mm}$

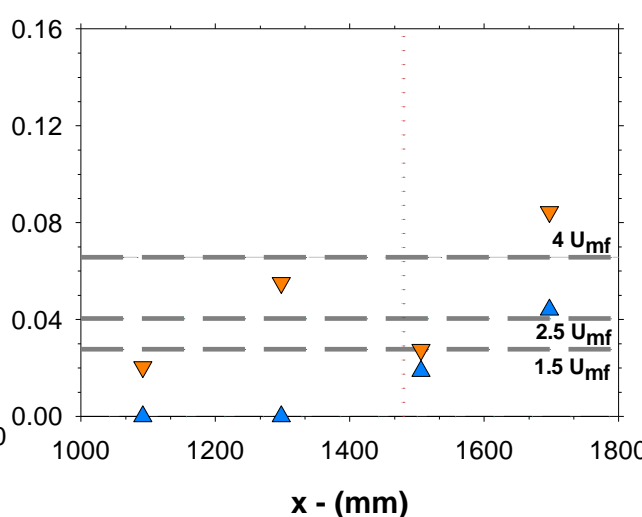
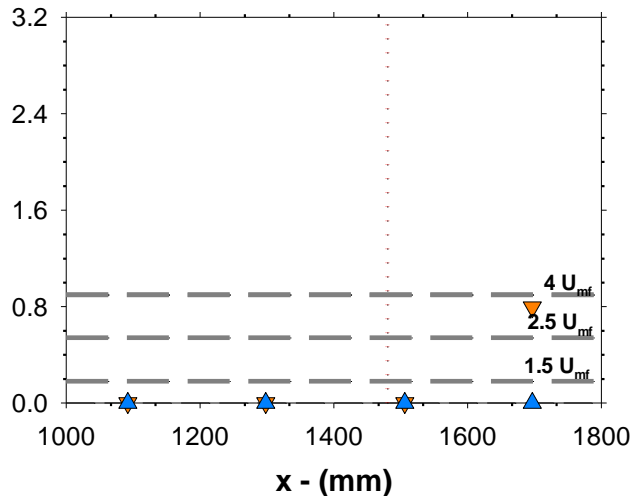
Mean bubble frequency - (Hz)



Local dispersion coefficient - (mm^2/s)



$h = 800\text{ mm}$



✓ the mobility of the dense phase is spatially correlated with the parameters of the bubble phase.

✓ fairly large values of D are observed even at locations where bubbly flow is not observed.

✓ enhanced solids mobility at locations where bubbles are not detected arises due to the establishment of coherent bed solids circulation of large correlation length promoted by uneven fluidization

Conclusions

- ❖ Results confirm the expected inherent tendency of the bed to equalize uneven fluidization.
- ❖ Crossflow of fluidizing gas from the active to the passive sections of the bed, driven by lateral pressure gradients, promotes fluidization of the passive section and/or defluidization of the active section of the bed.
- ❖ Crossflow becomes increasingly important as the bed depth increases and this makes compartmented fluidization of deep beds more problematic.
- ❖ Large scale coherent solids mobility is promoted also in the passive section of the bed by particle gulf streaming induced by bubbly flow in the active section.

See you at the Poster!

$$U_L = 0.66 U_{mf}$$
$$U_S = 2.5 U_{mf}$$

Thanks for your kind attention

